This article has been accepted for publication in IEEE Transactions on Vehicular Technology. This is the author's version which has not been fully edited and content may change prior to final publication. Citation information: DOI 10.1109/TVT.2024.3370094

Dynamic Output Feedback Fault-Tolerant Control for Switched Vehicle Active Suspension Delayed Systems

Zhenhua Li, Hongtian Chen, *Member, IEEE*, Wentao Wu, *Graduated Student Member, IEEE*, and Weidong Zhang, *Senior Member, IEEE*

***Abstract*—This paper considers the problem of dynamic output feedback fault-tolerant control for switched vehicle active suspension delayed systems with unknown measurement sensitivities. By utilizing a dynamic switched gain, a switched reduced-order state observer is designed to estimate unavailable system states and uncertain system parameters. Subsequently, based on the Nussbaum gain technique, an output feedback fault-tolerant control scheme is proposed to attenuate the influence of the unknown measurement sensitivity on the system output. In addition, an auxiliary switched system is constructed to make up for the effect of the actuator input delays and faults via the backstepping approach. It is proved that all the signals in the closed-loop switched system are semi-globally uniformly ultimate bounded. Meanwhile, the displacement of the vehicle body and the unsprung mass can remain within a small origin neighbourhood under a set of switching signals with average dwell time. Case studies are utilized to illustrate the flexibility and effectiveness of the proposed control approach and indicate that better stabilization of switched vehicle active suspension delayed systems can be achieved through the proposed adaptive fault-tolerant control strategy against the unknown measurement sensitivity.**

***Index Terms*—Switched vehicle active suspension delayed systems, dynamic output feedback control, fault-tolerant control, unknown measurement sensitivities, average dwell time.**

I. Introduction

The vehicle suspension system is regarded as a crucial component of a vehicle, enhancing overall stability and safety. It can be categorized into three following kinds: passive, semi-active, and active suspension. Among these, the vehicle active suspension system has gained significant attention in recent decades due to growing customer demands for enhanced vehicle performance [1]–[3]. At present, various control strategies for the vehicle active suspension system have been developed, such as the robust control [4], [5], the sliding mode control [6], and the adaptive control [7], [8]. However, the majority of proposed control schemes for vehicle active suspension systems assume the availability of real-time information from sensors, actuators, and controllers.

Currently, due to manufacturing constraints, sensor measurements in vehicle suspension systems may not always be available, leading to unmeasured system states. To overcome the limitations of state feedback control, researchers have explored output feedback control methods for vehicle suspension systems [9]–[12]. In [5], a dynamic output feedback controller was presented for a vehicle active suspension system under the H_∞ criteria, employing an event-triggered mechanism. In [9], the problem of output-feedback saturation control was addressed for quarter-car active suspensions using an adaptive neural network algorithm. A sensor fault accommodation strategy was proposed for the vehicle active suspensions by using the output feedback adaptive control in [11]. Based on the critic-actor framework, the optimal output-feedback controller was designed to solve the optimization for the vehicle active suspension system in [13]. However, the presence of unknown measurement sensitivity errors in sensors is inevitable, as sensors cannot be ideal. Thus, the conventional output feedback control strategies are no longer feasible for the stabilization of the vehicle suspension system. Furthermore, the aforementioned studies focused on full-order state observer-based output feedback control assuming ideal output measurements. With the limited electronic resources, it is expected to develop the output feedback control technique for the vehicle suspension system with the unknown measurement sensitivity through a reduced-order state observer.

Moreover, switched resistance-inductance electromagnetic actuators are valuable alternatives for vehicle active suspension systems due to their simplicity, cost-effectiveness, and enhanced control performance. Hence, the switched vehicle active suspension system comprises a vehicle active suspension system and a switched electromagnetic actuator under a set of switching signals transmitted over the controller area network (CAN) [14]. Designing an appropriate switching signal, including multiple Lyapunov functions, common Lyapunov function, average dwell time (ADT), mode-dependent ADT, and state-dependent switching law [15]–[22], is a crucial issue for switched systems. Since the potential switched actuator faults of vehicle active suspension systems may originate from the data transmission through the CAN and the external disturbance, the fault-tolerant ability of the control strategy for

This paper was supported in part by the National Key R&D Program of China under Grant 2022ZD0119900, in part by the Shanghai Science and Technology Program under Grant 22015810300, in part by the National Natural Science Foundation of China under Grants U2141234 and 62303308, in part by the Hainan Province Science and Technology Special Fund under Grant ZDYF2021GXJS041, in part by Shanghai Pujiang Program under Grant 23PJ1404700, and in part by the Hainan Special PhD Scientific Research Foundation of Sanya Yazhou Bay Science and Technology City under Grant HSPHDSRF-2022-01-005. (*Corresponding author: Weidong Zhang*.)

The authors are with the Department of Automation, Shanghai Jiao Tong University, Shanghai 200240, China, and with the Key Laboratory of System Control and Information Processing, Ministry of Education of China, Shanghai 200240, China. (e-mail: lizhenhuagd@163.com (Z. Li); hongtian.chen@sjtu.edu.cn (H. Chen); wentao-wu@sjtu.edu.cn (W. Wu); wdzhang@sjtu.edu.cn (W. Zhang)).

Authorized licensed use limited to: UNIVERSITY OF VICTORIA. Downloaded on February 27,2024 at 21:29:31 UTC from IEEE Xplore. Restrictions apply.
© 2024 IEEE. Personal use is permitted, but republication/redistribution requires IEEE permission. See https://www.ieee.org/publications/rights/index.html for more information.

This article has been accepted for publication in IEEE Transactions on Vehicular Technology. This is the author's version which has not been fully edited and content may change prior to final publication. Citation information: DOI 10.1109/TVT.2024.3370094

the vehicle active suspension systems is also an inessential issue to ensure the operation safety [23]–[25]. Especially, actuator faults can severely degrade vehicle performance and contribute to safety accidents [26]. Additionally, the backstepping technique is an effective control design approach to address the actuator fault issue for the vehicle active suspension systems. In [24], the non-fragile fault-tolerant control design was proposed for vehicle suspension active systems by taking into account input quantization. In [25], concerned with faults in the actuator and measurement, the fault-tolerant control was developed for the discrete-time vehicle active suspension based on a reduced-order observer.

With the rapidly increasing requirements in autonomous driving, the CAN, as an advanced communication protocol, produces better communication service in vehicle network tasks. However, it is unavoidable to suffer from time delays due to data transmission through the CAN [1]. Through the vehicle voltage signals, the vehicle intrusion detection systems were proposed under low-delay data transmission in [27]. It is often the case that time delays adversely affect the performance of the system actuator. Sometimes, they can even result in the instabilities of existing control systems [28]. Naturally, some challenging issues are raised as follows: Is it possible to solve the output feedback fault-tolerant control problem for the switched vehicle active suspension delayed system, where the unknown measurement sensitivity from the system output and the input delay from the system actuator occur simultaneously? What should be done to design the proper multiple Lyapunov functions and the dynamic reduced-order observer-based adaptive output feedback controllers when the random road surface excitation takes place under a set of switching signals?

Motivated by these facts, this study focuses on the output feedback fault-tolerant adaptive control with a dynamic switched reduced-order state observer for switched vehicle active suspension delayed systems with the unknown measurement sensitivity. The main contributions of this study are summarised as follows:

1) Different from the conventional full-order state observer techniques [11], [13], the switched reduced-order state observer is designed to estimate unavailable system states and deal with uncertain system parameters with a dynamic switched gain. It significantly reduces the closed-loop system's order, therefore improving computational efficiency and real-time performance.
2) The Nussbaum gain technique is applied to detect the unknown parameters produced via the unknown measurement sensitivity from the system output. For the auxiliary switched system, the effect of the actuator input delay can be weakened via the backstepping approach using the multiple Lyapunov functions.
3) Actuator faults and switched delayed electromagnetic systems are simultaneously considered in the vehicle active suspension systems. The dynamic output-feedback fault-tolerant control scheme is flexibly proposed to address the effects of actuator faults with a set of switching signals satisfying ADT.

In light of the current state of the art, the presented control scheme is discussed in more detail below. For vehicle active suspension delayed systems or non-switched ones, this paper takes the more general vehicle active suspension systems with input delays into account, while none of [4], [11], [29] considered actuator faults and unknown measurement sensitivity simultaneously. At present, for vehicle active suspension systems, the pioneers have developed a lot of state-feedback control strategies [2], [5], [7], while a few researchers have presented the output-feedback control method to estimate the unmeasurable states [10], [12]. However, when the vehicle active suspension systems have input delays and actuator faults under a switching signal, most of the existing control methods will no longer be suitable. Therefore, how to design an output-feedback controller to alleviate the impacts of input delays and actuator faults and to guarantee system stabilization is the motivation for this paper.

The remainder of this study is arranged as follows. Section II mainly includes the system description and the related knowledge. The control strategy and stability analysis are presented in Section III. Section IV demonstrates the effectiveness and flexibility of the proposed control scheme. The conclusions are drawn in Section V.

II. System Description

A. Switched Vehicle Active Suspension Delayed Systems

According to [4], [10], the switched vehicle active suspension delayed system over the CAN is depicted in Fig. 1. In fact, time delays often occur through the CAN. Inspired by [30], [31], the switched delayed electromagnetic system, as a typical hybrid system, has excellent performance under a suitable switching signal. Here, the switched vehicle active suspension delayed system consists of a vehicle active suspension system and a switched delayed electromagnetic actuator under a set of switching signals. Based on Newton's law and Kirchhoff's circuit law, the systems' dynamic differential equations are given by

$$\begin{cases} M_v \ddot{D}_s = -F_a - F_s + F_{Ue}, \\ M_u \ddot{D}_w = F_a + F_s - F_{wr} - F_{Ue}, \\ u_{\sigma(t)}(t - \tau(t)) = R_{\sigma(t)} i + L_{\sigma(t)} \dot{i}, \end{cases} \tag{1}$$

where a switching signal $\sigma(t)$ is a piecewise right continuous function with $\bar{k} \geq 2$ being the number of subsystems satisfying $\sigma(t) : [0, \infty) \to \Gamma = \{1, \ldots, \bar{k}\}$. During the time interval $[t_j, t_{j+1})$, the $\bar{k}_j$-th subsystem is active with the switching time instant t_j. The sprung mass and the unsprung mass are denoted as M_v and M_u, respectively. D_s and D_w express the absolute displacement of the sprung mass and the unsprung mass, respectively. D_r denotes the random road surface excitation. F_a and F_{wr} are the elastic forces, which are produced by the stiffness coefficients of the sprung mass and unsprung mass, respectively. F_s is the damping force produced by the stiffness coefficient of the sprung mass. Meanwhile, the output forces are denoted as $F_a = c_a(D_s - D_w)$, $F_s = c_s(\dot{D}_s - \dot{D}_w)$, and $F_{wr} = F_w + F_r$ with $F_w = c_w(D_w - D_r)$ and $F_r = c_r(\dot{D}_w - \dot{D}_r)$, where c_a, c_w and c_s, c_r are the stiffness coefficients and the damping coefficients, respectively. The

Authorized licensed use limited to: UNIVERSITY OF VICTORIA. Downloaded on February 27,2024 at 21:29:31 UTC from IEEE Xplore. Restrictions apply.
© 2024 IEEE. Personal use is permitted, but republication/redistribution requires IEEE permission. See https://www.ieee.org/publications/rights/index.html for more information.

This article has been accepted for publication in IEEE Transactions on Vehicular Technology. This is the author's version which has not been fully edited and content may change prior to final publication. Citation information: DOI 10.1109/TVT.2024.3370094

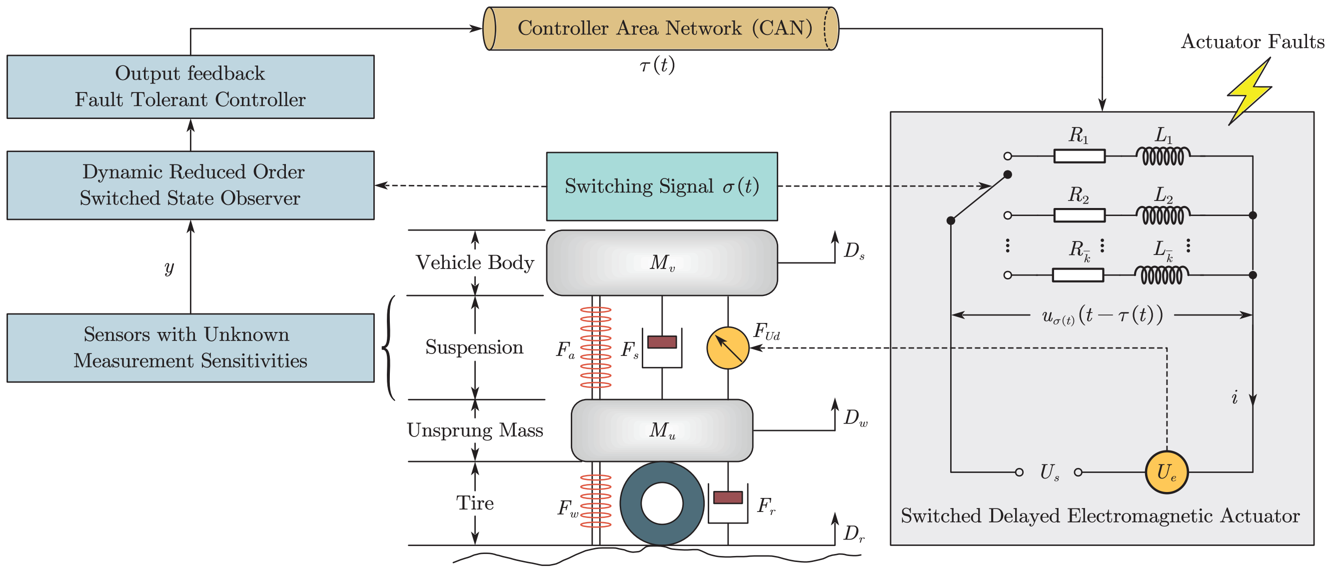

Fig. 1: The framework of switched vehicle active suspension delayed systems over the CAN.

back electromotive force, F_{Ue}, is produced by the voltage U_e and is given by $F_{Ue} = \frac{2\pi T_e}{P_e}$. In addition, $T_e = c_e i$ is the output torque of the permanent magnet motor, where c_e denotes the equivalent torque and i stands for the current. P_e expresses the guidance in the switched electromagnetic actuator. For $k \in \Gamma$, $u_k(t-\tau(t)) = U_s - U_e$ is the input signal through the transmission delays over the CAN, where U_s is the input voltage. $\tau(t)$ is the unknown time-varying delay. L_k and R_k denote the inductance and resistance of the switched electromagnetic actuator, respectively. In this case, $\Upsilon(t_0) = U_k(t_0)$ for $k \in \Gamma$ represents the input initial value at $t_0 \in [-\tau, 0]$.

Define the state variables as $x = [x_1, x_2, x_3]^\top$ with $x_1 = D_s - D_w$, $x_2 = \dot{D}_s - \dot{D}_w$, and $x_3 = \frac{2\pi c_e M}{P_e} i$, where $M = \frac{1}{M_v} + \frac{1}{M_u}$. In the actual situation, due to manufacturing reasons, the sensors cannot be ideal such that an unknown measurement sensitivity in the system output y exists. In addition, the system output y stands for the suspension space with unknown measurement sensitivity, i.e., the displacement bias between the sprung and unsprung mass. Then, the switched vehicle active suspension delayed system is represented as follows:

$$\begin{cases} \dot{x}_1 = x_2, \\ \dot{x}_2 = x_3 + f_2(x_2) + \vartheta h(y) + \frac{1}{M_u} F_{wr}, \\ \dot{x}_3 = g_{\sigma(t)} u_{\sigma(t)}(t-\tau(t)) + f_{3,\sigma(t)}(x_3), \\ y = \rho x_1, \end{cases} \tag{2}$$

Note that during $t \in [t_j, t_{j+1})$, one gets $\sigma(t) = k \in \Gamma$, where t_j and t_{j+1} are the time instant. $u_{\sigma(t)}(t-\tau(t))$ is the delayed actuator input. ρ is the completely unknown measurement sensitivity constant from the system output sensor satisfying $\rho \neq 0$ (its sign and size are both unknown). $f_2(x_2) = -Mc_s x_2$ and $f_{3,\sigma(t)}(x_3) = -\frac{R_{\sigma(t)}}{L_{\sigma(t)}} x_3$ are known functions. $\vartheta = -\frac{c_a}{\rho}$ is a uncertain parameter with unknown constants c_a and ρ. $h(y) = My$ is a known smooth function vector, $g_{\sigma(t)} = \frac{2\pi c_e M}{P_e L_{\sigma(t)}}$ is an unknown positive parameter with the unknown constants c_e and P_e.

In practice, the complex road surface excitation can fail the switched delayed electromagnetic actuator in (2). For $k \in \Gamma$, the fault model of the k-th addressed actuator input is considered as follows:

$$u_k(t) = \hbar_k v_k(t) + b_k(t), \;\; \forall t > t_s, \tag{3}$$

where $\hbar_k \in [0, 1]$ represents the unknown failure factor, $v_k(t)$ is the actual control input, $b(t)$ is an unknown bias fault satisfying $|b_k(t)| \leq \bar{b}_k$ with its upper bound $\bar{b}_k$, and t_s is the unknown time instant when the failure occurs. The actuator failure can be categorized into three patterns for $k \in \Gamma$:

1) If $\hbar_k = 1$ and $b_k(t) = 0$, then $u_k(t) = v_k(t)$, indicating that the k-th actuator works normally.
2) If $0 < \hbar_k < 1$ and $b_k(t) = 0$, then $u_k(t) = \hbar_k v_k(t)$, implying that the k-th actuator loses partial effectiveness.
3) If $\hbar_k = 0$ and $b_k(t) \neq 0$, then $u_k(t) = b_k(t)$, describing that the total effectiveness of the k-th actuator is lost.

Our control objective is to develop a dynamic reduced-order switched state observer-based output feedback fault-tolerant control scheme for switched vehicle active suspension delayed systems with unknown measurement sensitivities. The relative vertical displacement, the vertical velocity, and the electric current intensity can be stabilized by the proposed controller under a set of switching signals with ADT. Meanwhile, the ride comfort and driving safety for passengers can be improved regardless of any switched electromagnetic actuator input delays and failures.

Assumption 1 [6]: The uninterrupted contact from wheels to the road surface $D_w - D_r$ and its first order derivatives $\dot{D}_w - \dot{D}_r$ are continuous and bounded, satisfying $|D_w - D_r| \leq D_1$ and $|\dot{D}_w - \dot{D}_r| \leq D_2$.

Remark 1: Assumption 1 implies that the states D_w and D_r of the active suspension system are bounded due to the physical limitations of power capacity and structure in vehicle

Authorized licensed use limited to: UNIVERSITY OF VICTORIA. Downloaded on February 27,2024 at 21:29:31 UTC from IEEE Xplore. Restrictions apply.
© 2024 IEEE. Personal use is permitted, but republication/redistribution requires IEEE permission. See https://www.ieee.org/publications/rights/index.html for more information.

This article has been accepted for publication in IEEE Transactions on Vehicular Technology. This is the author's version which has not been fully edited and content may change prior to final publication. Citation information: DOI 10.1109/TVT.2024.3370094

systems from wheels to the road surface. It is commonly used when focusing on the stabilization for the active suspension system [9], [11], [13].

Definition 1 [20]: For the switched systems, a switching signal $\sigma(t)$ satisfying an ADT $\tau_a > 0$ holds that

$$N_\sigma(T,t) \leq N_0 + \frac{T-t}{\tau_a}, \ \forall T \geq t \geq 0, \tag{4}$$

where $N_\sigma(T,t)$ stands for the switching numbers on the time interval $[t,T]$ and $N_0 > 0$ is denoted as the chatter bounds.

Lemma 1 [32]: For $k \in \Gamma$, a symmetric matrix $P_k > 0$ and positive numbers ν_k, ϱ_k, $l_{2,k}$ and $l_{3,k}$ exist such that

$$A_k^\top P_k + P_k A_k \leq -\nu_k P_k, \tag{5}$$

$$-\varrho_k P_k \leq BP_k + P_k B \leq \varrho_k P_k, \tag{6}$$

where $A_k = \begin{bmatrix} -l_{2,k} & 1 \\ -l_{3,k} & 0 \end{bmatrix}$ is a Hurwitz matrix and $B = \mathrm{diag}\{0,1\}$.

B. Nussbaum Gain Technique Properties

Without a priori regarding the control gains, the Nussbaum gain technique will be employed to design the auxiliary subsystems in this paper. The Nussbaum gain function $\mathcal{N}(\chi)$ has two properties satisfying

$$\lim_{t\to\infty} \sup \frac{1}{t}\int_0^t \mathcal{N}(\chi)d\chi = +\infty, \tag{7a}$$

$$\lim_{t\to\infty} \inf \frac{1}{t}\int_0^t \mathcal{N}(\chi)d\chi = -\infty. \tag{7b}$$

Lemma 2 [33], [34]: Let $V(t) \geq 0$ and $\mathcal{N}(\chi)$ be the smooth functions over the time interval $[0, t_f)$. For Nussbaum gain functions $\mathcal{N}(\chi)$, one gets

$$V(t) \leq \pi_0 + e^{-at}\int_0^t \epsilon(s)(\mathcal{N}(\chi(s)) + 1)\dot{\chi}(s)e^{as}ds, \tag{8}$$

where π_0 and a are positive parameters, $t \in [0, t_f)$, and $\epsilon(\cdot)$ is a time-varying parameter satisfying $0 < \underline{\epsilon} \leq |\epsilon(\cdot)| \leq \bar{\epsilon}$ with the unknown constants $\underline{\epsilon}$ and $\bar{\epsilon}$ such that $\int_0^t \epsilon(s)(\mathcal{N}(\chi(s)) - 1)\dot{\chi}(s)e^{as}ds$, $\chi(t)$, and $V(t)$ are bounded over the time interval $[0, t_f)$.

Lemma 3 [35]: For the positive constant t_f on the interval $[t_0, t_f)$, if the solution of the closed-loop system is verified to be bounded, then one gets $t_f = +\infty$.

C. Radial Basis Function-Based Neural Network

The radial basis function-based neural network is considered as follows

$$\bar{f}_{NN}(X) = W^\top S(X) \in \mathbb{R}, \tag{9}$$

where the weight vector $W = [w_1, \ldots, w_\ell]^\top \in \mathbb{R}^\ell$ contains ℓ nodes whose number is greater than one, and its basic function vector $S(X) \in \mathbb{R}^\ell$ contains the input vector X. Meanwhile, the neural network can approximate the unknown continuous function satisfying with the following equation

$$\bar{f}(X) = W^{*\top} S(X) + \delta(X), \tag{10}$$

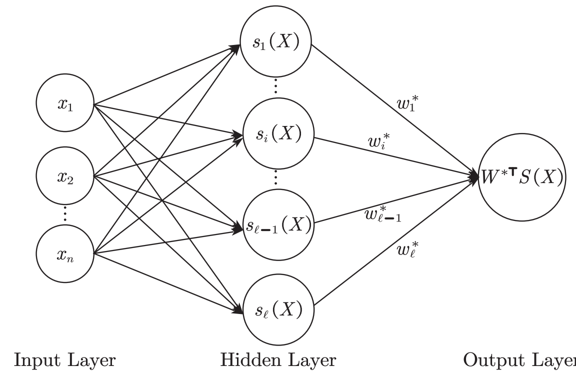

Fig. 2: The schematic of the neural network's estimation of unknown nonlinear functions.

where $X = [x_1, \ldots, x_n]^\top \in \mathbb{R}^n$ and $\delta(X)$ is the approximation error satisfying $|\delta(X)| \leq \delta^*$ with any given positive constant δ^*. In addition, $W^* = [w_1^*, \ldots, w_\ell^*]^\top \in \mathbb{R}^\ell$ demonstrates an ideal weight vector. Consider $S(X) = [s_1(X), \ldots, s_\ell(X)]^\top \in \mathbb{R}^\ell$ with the Gaussian functions $s_i(X)$ as follows for $i = 1, \ldots, \ell$,

$$s_i(X) = \exp\left[\frac{-(X-\vartheta_i)^\top (X-\vartheta_i)}{\iota^2}\right], \tag{11}$$

where ι is the width of the Gaussian function and $\vartheta_i = [\vartheta_{i1}, \ldots, \vartheta_{in}]^\top$ is the center. The schematic of the neural network's estimation of unknown nonlinear functions is shown in Fig. 2. For convenience, $\bar{f}(X)$ is denoted as $\bar{f}(X) = W^{*\top}S + \delta$ with

$$W^* := \arg\min_{W\in\mathbb{R}^\ell}\left\{\sup_{X\in\Omega}\left|\bar{f}(X) - \bar{f}_{NN}(X)\right|\right\}. \tag{12}$$

III. Main Results

By employing the multiple Lyapunov functions, for the switched vehicle active suspension delayed system (1), this section develops an adaptive output-feedback fault-tolerant control scheme with a dynamic reduced-order switched state observer-based via the backstepping method, and demonstrates the stability analysis of the closed-loop system under ADT.

A. Dynamic Reduced-Order Switched State Observer

Together with the inaccurate output information y and the delayed actuator input $u_k(t-\tau(t))$ in (2), the dynamic reduced-order switched state observer is designed to deal with the uncertain parameter ϑ as follows:

$$\begin{cases} \xi_i = \phi_i + l_{i,k}r^{i-1}y, \ i = 2, 3, \\ \dot{\phi}_2 = \xi_3 + f_2(\xi_2) - l_{2,k}r\xi_2 - l_{2,k}\dot{r}y, \\ \dot{\phi}_3 = f_{3,k}(\xi_3) - l_{3,k}r^2\xi_2 - 2l_{3,k}r\dot{r}y, \\ \dot{\varphi}_2 = \varphi_3 + f_2(\varphi_2) + h(y) - l_{2,k}r\varphi_2, \\ \dot{\varphi}_3 = f_{3,k}(\varphi_3) - l_{3,k}r^2\varphi_2, \\ \dot{\gamma}_2 = \gamma_3 + f_2(\gamma_2) - l_{2,k}r\gamma_2, \\ \dot{\gamma}_3 = u_k(t-\tau(t)) + f_{3,k}(\gamma_3) - l_{3,k}r^2\gamma_2, \end{cases} \tag{13}$$

Authorized licensed use limited to: UNIVERSITY OF VICTORIA. Downloaded on February 27,2024 at 21:29:31 UTC from IEEE Xplore. Restrictions apply.
© 2024 IEEE. Personal use is permitted, but republication/redistribution requires IEEE permission. See https://www.ieee.org/publications/rights/index.html for more information.

This article has been accepted for publication in IEEE Transactions on Vehicular Technology. This is the author's version which has not been fully edited and content may change prior to final publication. Citation information: DOI 10.1109/TVT.2024.3370094

where for $k \in \Gamma$, $\xi = [\xi_2, \xi_3]^\top$, $\varphi = [\varphi_2, \varphi_3]^\top$ and $\gamma = [\gamma_2, \gamma_3]^\top$ are the state variables of the switched reduced-order state observer (13), produced by the measurable states y and $u_k(t-\tau(t))$. $f_2(*_2)$ and $f_{3,k}(*_3)$ with $* = \xi, \varphi, \gamma$ are the same definition in (2). r is a dynamic switched gain to be designed later with $r(0) = 1$.

To proceed with, based on the state variables ξ, φ and γ in (13), the estimated states for the system (2) are constructed as

$$\begin{cases} \hat{x}_2 = \frac{1}{\rho}\xi_2 + \vartheta\varphi_2 + g_k\gamma_2, \\ \hat{x}_3 = \frac{1}{\rho}\xi_3 + \vartheta\varphi_3 + g_k\gamma_3 \end{cases} \tag{14}$$

with $\hat{x} = [\hat{x}_2, \hat{x}_3]^\top$, where $\hat{x}_i$ for $i = 2, 3$ are the estimation of x_i. Then, the error of the reduced-order state observer estimator is defined as

$$\tilde{\varepsilon}_i = (x_i - \hat{x}_i) \tag{15}$$

and $\tilde{\varepsilon} = [\tilde{\varepsilon}_2, \tilde{\varepsilon}_3]^\top$. Based on (2) and (13)-(15), one has

$$\begin{cases} \dot{\tilde{\varepsilon}}_2 = \tilde{\varepsilon}_3 + f_2(\tilde{\varepsilon}_2) - l_{2,k} r\tilde{\varepsilon}_2 + \frac{1}{M_u}F_{wr}, \\ \dot{\tilde{\varepsilon}}_3 = f_{3,k}(\tilde{\varepsilon}_3) - l_{3,k} r^2\tilde{\varepsilon}_2. \end{cases} \tag{16}$$

Then, the scaling transformation for the estimated error dynamics system is defined as

$$\varepsilon_i = r^{2-i-\varrho_k}\tilde{\varepsilon}_i, \ i = 2, 3 \tag{17}$$

with $\varepsilon = [\varepsilon_2, \varepsilon_3]^\top$, where ϱ_k is defined in Lemma 1. Based on (16) and (17), one gets

$$\dot{\varepsilon} = rA_k\varepsilon - \frac{\dot{r}}{r}B_k\varepsilon - \varrho_k\frac{\dot{r}}{r}\varepsilon + F_{1,k} + F_{2,k}, \tag{18}$$

where A_k and B_k are defined in Lemma 1, $F_{1,k} = [r^{-\varrho_k}f_2(\tilde{\varepsilon}_2), r^{-1-\varrho_k}f_{3,k}(\tilde{\varepsilon}_3)]^\top = [-Mc_s\varepsilon_2, -\frac{R_k}{L_k}\varepsilon_3]^\top$, and $F_{2,k} = [\frac{r^{-\varrho_k}}{M_u}F_{wr}, 0]^\top$. The Lyapunov candidate function is considered as follows:

$$V_\varepsilon = \varepsilon^\top P_k\varepsilon. \tag{19}$$

Then, the time derivative of V_ε along with the estimated error dynamics system (18) is

$$\begin{aligned} \dot{V}_\varepsilon = {} & r\varepsilon^\top(A_k^\top P_k + P_kA_k)\varepsilon - \frac{\dot{r}}{r}\varepsilon^\top(BP_k + P_kB + \varrho_kP_k)\varepsilon \\ & + 2\varepsilon^\top P_k(F_{1,k} + F_{2,k}) - \varrho_k\frac{\dot{r}}{r}\varepsilon^\top P_k\varepsilon. \end{aligned} \tag{20}$$

Based on (2), (17), and Young's inequality, one has

$$\begin{aligned} 2\varepsilon^\top P_kF_{1,k} & \le \bar{\lambda}(P_k)\varepsilon^\top P_k\varepsilon + \|F_{1,k}\|^2 \\ & \le \bar{\lambda}(P_k)\varepsilon^\top P_k\varepsilon + M^2c_s^2\varepsilon_2^2 + \frac{R_k^2}{L_k^2}\varepsilon_3^2 \\ & \le \bar{\lambda}(P_k)\varepsilon^\top P_k\varepsilon + \frac{M^2c_s^2}{\underline{\lambda}(P_k)}\varepsilon^\top P_k\varepsilon + \frac{R_k^2\varepsilon^\top P_k\varepsilon}{L_k^2\underline{\lambda}(P_k)}, \end{aligned} \tag{21}$$

$$2\varepsilon^\top P_kF_{2,k} \le \bar{\lambda}(P_k)\varepsilon^\top P_k\varepsilon + \|F_{2,k}\|^2, \tag{22}$$

where $\bar{\lambda}(P_k)(\underline{\lambda}(P_k))$ stand for the largest (smallest) eigenvalue of the matrix P_k for $k \in \Gamma$, respectively. According to (21), (22), and Lemma 1, one gets

$$\begin{aligned} \dot{V}_\varepsilon \le {} & -r\nu_k\varepsilon^\top P_k\varepsilon - \frac{\dot{r}}{r}\varepsilon^\top(BP_k + P_kB + \varrho_kP_k)\varepsilon + \|F_{2,k}\|^2 \\ & + \psi_k\varepsilon^\top P_k\varepsilon + \bar{\lambda}(P_k)\varepsilon^\top P_k\varepsilon - \varrho_k\frac{\dot{r}}{r}\varepsilon^\top P_k\varepsilon. \end{aligned} \tag{23}$$

where $\psi_k = \bar{\lambda}(P_k) + \frac{M^2c_s^2}{\underline{\lambda}(P_k)} + \frac{R_k^2}{L_k^2\underline{\lambda}(P_k)}$. Meanwhile, the dynamic switched gain $r(t)$ is designed as

$$\dot{r}(t) = \max_{k\in\Gamma}\left\{-\frac{r}{\varrho_k}\left(\omega_kr - \psi_k - \bar{\lambda}(P_k) - \frac{\varsigma}{\underline{\lambda}(P_k)}\right), 0\right\}, \tag{24}$$

where $\omega_k < \nu_k$ and ς are positive parameters and $r(0) = 1$. Inspired by [36], it can be deduced from (24) that r and $\dot{r}$ are bounded satisfying $1 \le r \le \bar{r}$, where the constant $\bar{r}$ is the upper bound of r. In addition, based on (1) and Assumption 1, one obtains

$$\begin{aligned} \|F_{2,k}\|^2 & = \frac{\bar{r}^{-2\varrho_k}}{M_u^2}F_{wr}^2 = \frac{\bar{r}^{-2\varrho_k}}{M_u^2}(F_w + F_r)^2 \\ & \le \frac{\bar{r}^{-2\varrho_k}}{M_u^2}\left[2c_w^2(D_w - D_r)^2 + 2c_r^2(\dot{D}_w - \dot{D}_r)^2\right] \\ & \le \frac{2\bar{r}^{-2\varrho_k}}{M_u^2}(c_w^2D_1^2 + c_r^2D_2^2). \end{aligned} \tag{25}$$

By substituting (24) and (25) into (23), one has

$$\dot{V}_\varepsilon \le -\underline{\omega}_k\varepsilon^\top P_k\varepsilon - \varsigma\|\varepsilon\|^2 + \delta_{0,k}, \tag{26}$$

where $\underline{\omega}_k$ and $\delta_{0,k}$ are positive constants defined as $\underline{\omega}_k = \nu_k - \omega_k$ and $\delta_{0,k} = \frac{2\bar{r}^{-2\varrho_k}}{M_u^2}(c_w^2D_1^2 + c_r^2D_2^2)$, respectively.

B. Output Feedback Fault-Tolerant Controller Design

Firstly, an auxiliary switched system is designed to compensate for the influence of the actuator input delay as follows:

$$\begin{cases} \dot{\varpi}_i = \varpi_{i+1} - d_{i,\sigma(t)}\varpi_i, \ i = 1, 2, \\ \dot{\varpi}_3 = -d_{3,\sigma(t)}\varpi_3 + u_{\sigma(t)}(t - \tau(t)) - u_{\sigma(t)}(t), \end{cases} \tag{27}$$

where $\sigma(t)$ is a switching signal. ϖ_i and $d_{i,\sigma(t)}$ for $i = 1, 2, 3$ are the auxiliary switched system states and positive designed parameters, respectively. In addition, according to the backstepping approach, the following changes of a coordinate for all subsystems are defined as

$$\begin{cases} z_1 = y - \varpi_1, \\ z_i = \gamma_i - \alpha_{i-1} - \varpi_i, \ i = 2, 3, \end{cases} \tag{28}$$

where z_i for $i = 1, 2, 3$ is the errors of the coordinate transformation and α_{i-1} for $i = 2, 3$ stands for the virtual control inputs. As a matter of convenience, the unknown ideal value is expressed as

$$\theta_i^* = \max_{k\in M}\left\{\|W_{i,k}^*\|^2\right\}, \tag{29}$$

where $i = 0, 1, 2, \ldots, n$, $W_{i,k}^*$ stands for the ideal constant weight vector; meanwhile, $\tilde{\theta}_i$ is the estimation error satisfying $\tilde{\theta}_i = \theta_i^* - \hat{\theta}_i$, and $\hat{\theta}_i$ is the estimation of θ_i^*. Then, the detailed design process of the control scheme is shown in the following steps.

Initial Step: Based on (2), (14), (15), (17), and (27), one gets

$$\dot{z}_1 = \rho\left(\tilde{\varepsilon}_2 + \frac{1}{\rho}\xi_2 + \vartheta\varphi_2 + g_k\gamma_2\right) - \varpi_2 + d_{1,k}\varpi_1.$$

Authorized licensed use limited to: UNIVERSITY OF VICTORIA. Downloaded on February 27,2024 at 21:29:31 UTC from IEEE Xplore. Restrictions apply.
© 2024 IEEE. Personal use is permitted, but republication/redistribution requires IEEE permission. See https://www.ieee.org/publications/rights/index.html for more information.

This article has been accepted for publication in IEEE Transactions on Vehicular Technology. This is the author's version which has not been fully edited and content may change prior to final publication. Citation information: DOI 10.1109/TVT.2024.3370094

The Lyapunov function is considered as follows:

$$V_{1,k} = \frac{1}{2}z_1^2 + \frac{1}{2\ell_1}\tilde{\theta}_1^\top\tilde{\theta}_1 + V_\varepsilon, \tag{30}$$

where for $k \in \Gamma$, ℓ_1 is a positive constant. To proceed with (28), one obtains

$$\begin{aligned}\dot{V}_{1,k} = &\rho z_1\left[\tilde{\varepsilon}_2 + \frac{1}{\rho}\xi_2 + \vartheta\varphi_2 + g_k(z_2 + \alpha_1 + \varpi_2)\right]\\ &- \varpi_2 z_1 + d_{1,k}\varpi_1 z_1 - \frac{1}{\ell_1}\tilde{\theta}_1^\top\dot{\hat{\theta}}_1 + \dot{V}_\varepsilon.\end{aligned} \tag{31}$$

By using Young's inequality and (17), it can be obtained

$$\rho z_1\tilde{\varepsilon}_2 \le \frac{1}{4\varsigma}\rho^2 r^{2\varrho_k} z_1^2 + \varsigma\|\varepsilon\|^2. \tag{32}$$

Then, $\bar{f}_{1,k}(X_1) = \rho(\frac{1}{4\varsigma_1}\rho r^{2\varrho_k}z_1 + \vartheta\varphi_2) + \xi_2 + (\rho g_k - 1)\varpi_2$ is denoted as the uncertain continuous function with $X_1 = [z_1, r, \xi_2, \varphi_2, \varpi_2]^\top$. Based on (10)-(12), it induces

$$\bar{f}_{1,k}(X_1) = W_{1,k}^{*\top}S_1 + \delta_{1,k}, \tag{33}$$

where $\delta_{1,k}$ is the approximation error with $|\delta_{1,k}| < \delta_1^*$ and δ_1^* is a positive constant. Based on (29), (33), and Young's inequality, one obtains

$$z_1\bar{f}_{1,k}(X_1) \le \frac{1}{2a_1^2}z_1^2\theta_1^* S_1^\top S_1 + \frac{1}{2}a_1^2 + \frac{1}{2}z_1^2 + \frac{1}{2}\delta_1^{*2}, \tag{34}$$

where a_1 is a positive constant. Since ρ and g_k are respectively the unknown measurement sensitivity and the unknown control gain term, it is difficult to handle with the existing typical backstepping approach. Thus, a Nussbaum gain $\mathcal{N}(\chi_1)$ is utilized to deal with the issue from the unknown coefficients in the initial step. Furthermore, the virtual controller input α_1 and the adaptive law $\dot{\hat{\theta}}_1$ can be considered as

$$\alpha_1 = \mathcal{N}(\chi_1)(c_1 z_1 + \Xi_1), \tag{35}$$

$$\dot{\hat{\theta}}_1 = \frac{\ell_1}{2a_1^2}z_1^2 S_1^\top S_1 - \kappa_1\hat{\theta}_1 \tag{36}$$

with $\Xi_1 = \frac{1}{2a_1^2}z_1\hat{\theta}_1 S_1^\top S_1 + \frac{1}{2}z_1 + d_{1,k}\varpi_1$, where c_1 and κ_1 are positive constants. Meanwhile, the related control designs using the Nussbaum-type technique are as follows:

$$\mathcal{N}(\chi_1) = e^{\chi_1^2}\cos\chi_1,\ \dot{\chi}_1 = c_1 z_1^2 + \Xi_1 z_1. \tag{37}$$

Substituting (48)-(37) into (31) obtains

$$\begin{aligned}\dot{V}_{1,k} \le &- \underline{\omega}_k\varepsilon^\top P_k\varepsilon + \frac{\kappa_1}{\ell_1}\tilde{\theta}_1^\top\hat{\theta}_1 - c_1 z_1^2 + \Theta_{1,k}\\ &+ (\rho g_k\mathcal{N}(\chi_1) + 1)\dot{\chi}_1 + \rho g_k z_1 z_2,\end{aligned} \tag{38}$$

where $\Theta_{1,k} = \delta_{0,k} + \frac{1}{2}a_1^2 + \frac{1}{2}\delta_1^{*2}$.

Step 2: Based on (13), (27), and (28), one has

$$\dot{z}_2 = \gamma_3 + f_2(\gamma_2) - l_{2,k}r\gamma_2 - \dot{\alpha}_1 - \varpi_3 + d_{2,k}\varpi_2.$$

The Lyapunov function can be constructed by

$$V_{2,k} = \frac{1}{2}z_2^2 + \frac{1}{2\ell_2}\tilde{\theta}_2^\top\tilde{\theta}_2 + V_{1,k}, \tag{39}$$

where ℓ_2 is a positive parameter. Furthermore, it is deduced from (28) that

$$\begin{aligned}\dot{V}_{2,k} = &z_2(z_3 + \alpha_2 + f_2(\gamma_2) - l_{2,k}r\gamma_2 - \dot{\alpha}_1 + d_{2,k}\varpi_2)\\ &- \frac{1}{\ell_2}\tilde{\theta}_2^\top\dot{\hat{\theta}}_2 + \dot{V}_{1,k}.\end{aligned} \tag{40}$$

Similar to the initial step, the uncertain functions are considered as $\bar{f}_{2,k}(X_2) = f_2(\gamma_2) - l_{2,k}r\gamma_2 - \dot{\alpha}_1 + \rho g_k z_1$ with $X_2 = [\gamma_2, r, \chi_1, y, \hat{\theta}_1, \varpi_1]^\top$ and $\dot{\alpha}_1 = \frac{\partial\alpha_1}{\partial\chi_1}\dot{\chi}_1 + \frac{\partial\alpha_1}{\partial y}\dot{y} + \frac{\partial\alpha_1}{\partial\hat{\theta}_1}\dot{\hat{\theta}}_1 + \frac{\partial\alpha_1}{\partial\varpi_1}\dot{\varpi}_1$. Based on (10)-(12), the neural network approximation is satisfied by

$$\bar{f}_{2,k}(X_2) = W_{2,k}^{*\top}S_2 + \delta_{2,k}, \tag{41}$$

where the error of approximation $\delta_{2,k}$ is satisfied by $|\delta_{2,k}| < \delta_2^*$ with positive parameter δ_2^*.

Through Young's inequality, (29), and (41), one has

$$z_2\bar{f}_{2,k}(X_2) \le \frac{1}{2a_2^2}z_2^2\theta_2^* S_2^\top S_2 + \frac{1}{2}a_2^2 + \frac{1}{2}z_2^2 + \frac{1}{2}\delta_2^{*2}, \tag{42}$$

where a_2 is the positive designed parameter. Meanwhile, the virtual controller input α_2 and the adaptive law $\dot{\hat{\theta}}_2$ are considered as

$$\alpha_2 = -c_2 z_2 - \Xi_2, \tag{43}$$

$$\dot{\hat{\theta}}_2 = \frac{\ell_2}{2a_2^2}z_2^2 S_2^\top S_2 - \kappa_2\hat{\theta}_2 \tag{44}$$

with $\Xi_2 = \frac{1}{2a_2^2}z_2\hat{\theta}_2 S_2^\top S_2 + \frac{1}{2}z_2 + d_{2,k}\varpi_2$, where c_2 and κ_2 are positive constants.

Substituting (41)-(44) into (40) obtains

$$\begin{aligned}\dot{V}_{2,k} \le &- \underline{\omega}_k\varepsilon^\top P_k\varepsilon + \sum_{i=1}^{2}\left(\frac{\kappa_i}{\ell_i}\tilde{\theta}_i^\top\hat{\theta}_i - c_i z_i^2\right) + \Theta_{2,k}\\ &+ (\rho g_k\mathcal{N}(\chi_1) + 1)\dot{\chi}_1 + z_2 z_3,\end{aligned} \tag{45}$$

where $\Theta_{2,k} = \Theta_{1,k} + \frac{1}{2}a_2^2 + \frac{1}{2}\delta_2^{*2}$.

Step 3: From (3), (13), (27), and (28), one can obtain

$$\dot{z}_3 = f_{3,k}(\gamma_3) - l_{3,k}r^2\gamma_2 - \dot{\alpha}_2 + d_{3,k}\varpi_3 + \hbar_k v_k(t) + b_k(t).$$

Let the Lyapunov function candidate be

$$V_{3,k} = \frac{1}{2}z_3^2 + \frac{1}{2\ell_3}\tilde{\theta}_3^\top\tilde{\theta}_3 + V_{2,k}, \tag{46}$$

where ℓ_3 is a positive constant. Similar to the procedure from (31) to (38), it yields

$$\begin{aligned}\dot{V}_{3,k} = &z_3(f_{3,k}(\gamma_3) - l_{3,k}r^2\gamma_2 - \dot{\alpha}_2 + d_{3,k}\varpi_3\\ &+ \hbar_k v_k(t) + b_k(t)) - \frac{1}{\ell_3}\tilde{\theta}_3^\top\dot{\hat{\theta}}_3 + \dot{V}_{2,k}.\end{aligned} \tag{47}$$

By utilizing Young's inequality and (3), one has

$$z_3 b_k(t) \le \frac{1}{2}z_3^2 + \frac{1}{2}\bar{b}_k^2. \tag{48}$$

To proceed, $\bar{f}_{3,k}(X_3) = f_{3,k}(\gamma_3) - l_{3,k}r^2\gamma_2 - \dot{\alpha}_2 + z_2$ is expressed as the uncertain function with $X_3 = [\gamma_2, \gamma_3, r, \chi_1, y, \hat{\theta}_1, \hat{\theta}_2, \varpi_2, \varpi_3]^\top$ and $\dot{\alpha}_2 = \frac{\partial\alpha_2}{\partial\chi_1}\dot{\chi}_1 + \frac{\partial\alpha_2}{\partial y}\dot{y} + \frac{\partial\alpha_2}{\partial\gamma_2}\dot{\gamma}_2 + \frac{\partial\alpha_2}{\partial\hat{\theta}_1}\dot{\hat{\theta}}_1 + \frac{\partial\alpha_2}{\partial\hat{\theta}_2}\dot{\hat{\theta}}_2 + \frac{\partial\alpha_2}{\partial\varpi_1}\dot{\varpi}_1 + \frac{\partial\alpha_2}{\partial\varpi_2}\dot{\varpi}_2$. Based on (10)-(12), the neural network approximation is given by

$$\bar{f}_{3,k}(X_n) = W_{3,k}^{*\top}S_3 + \delta_{3,k}, \tag{49}$$

Authorized licensed use limited to: UNIVERSITY OF VICTORIA. Downloaded on February 27,2024 at 21:29:31 UTC from IEEE Xplore. Restrictions apply.
© 2024 IEEE. Personal use is permitted, but republication/redistribution requires IEEE permission. See https://www.ieee.org/publications/rights/index.html for more information.

This article has been accepted for publication in IEEE Transactions on Vehicular Technology. This is the author's version which has not been fully edited and content may change prior to final publication. Citation information: DOI 10.1109/TVT.2024.3370094

where $\delta_{3,k}$ is the approximation error and a positive constant δ_3^* is satisfied by $|\delta_{3,k}| < \delta_3^*$. Based on Young's inequality, (29), and (49), it yields

$$z_3\bar{f}_{3,k}(X_3) \leq \frac{1}{2a_3^2}z_3^2\theta_3^* S_3^\top S_3 + \frac{1}{2}a_3^2 + \frac{1}{2}z_3^2 + \frac{1}{2}\delta_3^{*2}, \quad (50)$$

where a_3 is a positive parameter.

Then, a Nussbaum gain $\mathcal{N}(\chi_3)$ is utilized to deal with the unknown coefficients $\hbar_k$. To proceed with, the actual controller input v_k and the adaptive laws $\dot{\hat{\theta}}_3$ can be considered as

$$v_k = \mathcal{N}(\chi_3)(c_3 z_3 + \Xi_3), \quad (51)$$

$$\dot{\hat{\theta}}_3 = \frac{\ell_1}{2a_3^2}z_3^2 S_3^\top S_3 - \kappa_3\hat{\theta}_3 \quad (52)$$

with $\Xi_3 = \frac{1}{2a_3^2}z_3\hat{\theta}_3 S_3^\top S_3 + \frac{1}{2}z_3 + d_{3,k}\varpi_3$, where c_3 and κ_3 are positive constants. Meanwhile, the related control designs using the Nussbaum-type technique are as follows:

$$\mathcal{N}(\chi_3) = e^{\chi_3^2}\cos\chi_3,\ \dot{\chi_3} = c_3 z_3^2 + \Xi_3 z_3. \quad (53)$$

Combining (47)-(53) results in

$$\begin{aligned}\dot{V}_{3,k} \leq& \sum_{i=1}^{3}\left(\frac{\kappa_i}{\ell_i}\tilde{\theta}_i^\top\hat{\theta}_i - c_i z_i^2 + \bar{\mathcal{N}}(\chi_i)\dot{\chi_i}\right)\\ &- \underline{\omega}_k\varepsilon^\top P_k\varepsilon + \Theta_{3,k}, \end{aligned} \quad (54)$$

where $\bar{\mathcal{N}}(\chi_1) = \rho g_k\mathcal{N}(\chi_1) + 1$, $\bar{\mathcal{N}}(\chi_2) = 0$ with $\chi_2 = 0$, $\bar{\mathcal{N}}(\chi_3) = \hbar_k\mathcal{N}(\chi_3) + 1$, and $\Theta_{3,k} = \Theta_{2,k} + \frac{1}{2}a_3^2 + \frac{1}{2}\delta_3^{*2} + \frac{1}{2}\bar{b}_k^2$.

C. Stability Analysis

For notational convenience, the following definitions are used:

$$\mu = \min_{k\in\Gamma}\left\{\frac{\underline{\omega}_k\underline{\lambda}(P_k)}{\bar{\lambda}(P_k)}, 2c_i, \kappa_i, 2\ell_{i,k}, i = 1,2,3\right\}, \quad (55)$$

$$\zeta = \max\left\{\frac{\bar{\lambda}(P_k)}{\underline{\lambda}(P_p)},\ k,p\in\Gamma\right\}. \quad (56)$$

It is clear that $\mu > 0$ and $\zeta \geq 1$ are the two known parameters by suitably selecting P_k, $\underline{\omega}_k$, c_i, κ_i and $\ell_{i,k}$. The main theorem in this paper is summarized as follows.

Theorem 1: Consider the switched vehicle active suspension delayed system (1) satisfying Assumptions 1. The output feedback fault-tolerant controller (51) with the virtual controllers (35), (43), the dynamic reduced-order switched state observer (13), and the adaptive laws (36), (44), (52) can ensure all the closed-loop signals achieve semi-globally uniformly ultimate bounded. Meanwhile, the system output y with the unknown measurement sensitivity can stay in the small neighbourhood of zero under a set of switching signals with ADT. The block diagram of the proposed control scheme is depicted in Fig. 3.

Proof: The proof is divided into two parts to analyse the boundedness of all the signals in the closed-loop system. In part 1), the semi-global stability is verified for the switched vehicle active suspension delayed system with a set of switching signals satisfying ADT. In part 2), the system output y with the unknown measurement sensitivity is verified to stay in the small origin neighbourhood.

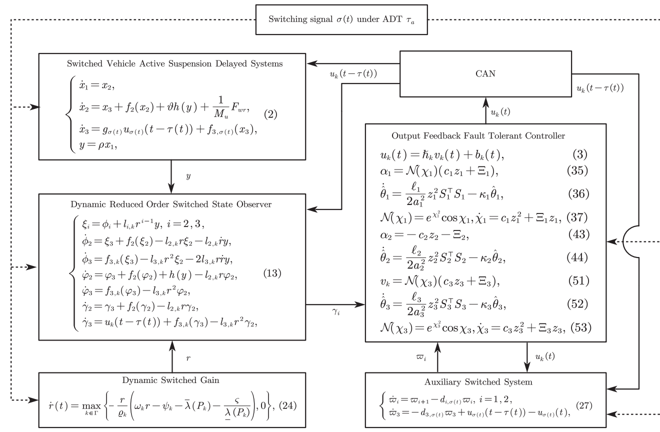

Fig. 3: The block diagram of the proposed control scheme.

1) To analyze the stability of the auxiliary switched system (27), the following Lyapunov function is constructed as

$$V_\varpi = \frac{1}{2}\sum_{i=1}^{3}\varpi_i^2. \quad (57)$$

Then, one gets

$$\begin{aligned}\dot{V}_\varpi =& \varpi_3(-d_{3,k}\varpi_3 + u_k(t-\tau(t)) - u_k(t))\\ &+ \sum_{i=1}^{2}\varpi_i(\varpi_{i+1} - d_{i,k}\varpi_i). \end{aligned} \quad (58)$$

Similar to the result in [37], $|u_k(t-\tau(t)) - u_k(t)| \leq u_k^*$ can be approached with a positive constant u_k^* for $k\in\Gamma$. Then, by using Young's inequality, one obtains

$$\begin{aligned}\dot{V}_\varpi \leq& -\sum_{i=1}^{3}d_{i,k}\varpi_i^2 + \sum_{i=1}^{2}\varpi_i\varpi_{i+1} + \varpi_3 u_k^*\\ \leq& -\sum_{i=1}^{3}\ell_{i,k}\varpi_i^2 + \frac{1}{2}u_k^*, \end{aligned} \quad (59)$$

where $\ell_{i,k}$ for $i = 1,2,3$ is a positive parameter satisfying $\ell_{1,k} = d_{1,k} - \frac{1}{2}$, $\ell_{2,k} = d_{2,k} - 1$, and $\ell_{3,k} = d_{3,k} - 1$. Here, based on (19), (30), (39), (46), and (57), the following multiple Lyapunov functions for $k\in\Gamma$ are constructed by

$$V_k(X) = \varepsilon^\top P_k\varepsilon + \frac{1}{2}\sum_{i=1}^{3}\left(z_i^2 + \frac{1}{\ell_i}\tilde{\theta}_i^\top\tilde{\theta}_i + \varpi_i^2\right), \quad (60)$$

where $X = [\varepsilon_2, \varepsilon_3, \tilde{\theta}_1, \tilde{\theta}_2, \tilde{\theta}_3, \varpi_1, \varpi_2, \varpi_3, z_1, z_2, z_3]^\top$. It is clear from (60) that two $\mathcal{K}_\infty$ functions $\underline{\alpha}(\|X\|)$ and $\overline{\alpha}(\|X\|)$ exist and hold that

$$\underline{\alpha}(\|X\|) \leq V_k(X) \leq \overline{\alpha}(\|X\|). \quad (61)$$

In addition, based on (56), it induces

$$V_k(X) \leq \zeta V_p(X),\ k,p\in\Gamma. \quad (62)$$

Furthermore, it yields

$$\dot{V}_k \leq \sum_{i=1}^{3}\left(\frac{\kappa_i}{\ell_i}\tilde{\theta}_i^\top\hat{\theta}_i - c_i z_i^2 - \ell_{i,k}\varpi_i^2 + \bar{\mathcal{N}}(\chi_i)\dot{\chi_i}\right)$$

Authorized licensed use limited to: UNIVERSITY OF VICTORIA. Downloaded on February 27,2024 at 21:29:31 UTC from IEEE Xplore. Restrictions apply.
© 2024 IEEE. Personal use is permitted, but republication/redistribution requires IEEE permission. See https://www.ieee.org/publications/rights/index.html for more information.

This article has been accepted for publication in IEEE Transactions on Vehicular Technology. This is the author's version which has not been fully edited and content may change prior to final publication. Citation information: DOI 10.1109/TVT.2024.3370094

$$-\underline{\omega}_k\varepsilon^\top P_k\varepsilon+\Theta_{3,k}+\frac{1}{2}u_k^*. \tag{63}$$

Meanwhile, the terms $\frac{\kappa_i}{\ell_i}\tilde{\theta}_i^\top\hat{\theta}_i$ from (63) satisfies

$$\frac{\kappa_i}{\ell_i}\tilde{\theta}_i^\top\hat{\theta}_i\leq\frac{\kappa_i}{2\ell_i}\theta_i^{*2}-\frac{\kappa_i}{2\ell_i}\tilde{\theta}_i^\top\tilde{\theta}_i, \tag{64}$$

According to (63)-(64), one has

$$\begin{aligned}\dot{V}_k\leq&-\sum_{i=1}^{3}\left(\frac{\kappa_i}{2\ell_i}\tilde{\theta}_i^\top\tilde{\theta}_i+c_iz_i^2+\ell_{i,k}\varpi_i^2-\bar{\mathcal{N}}(\chi_i)\dot{\chi}_i\right)\\&-\underline{\omega}_k\varepsilon^\top P_k\varepsilon+\Theta\\\leq&-\mu V_k+\sum_{i=1}^{3}\bar{\mathcal{N}}(\chi_i)\dot{\chi}_i+\Theta,\end{aligned} \tag{65}$$

where $\Theta=\max_{k\in\Gamma}\{\Theta_{3,k}+\frac{1}{2}u_k^*+\sum_{i=1}^{3}\frac{\kappa_i}{2\ell_i}\theta_i^{*2}\}$.

Let the initial time be $t_0=0$. Define the each switching time as $t_1,t_2,\ldots,t_{N_\sigma(T,0)}$ on the instant $[0,T]$ for $\forall T\geq 0$. Consider the function $\Phi(t)=e^{\mu t}V_{\sigma(t)}(X(t))$. Based on (65), one has $\dot{\Phi}(t)\leq\Theta e^{\mu t}+e^{\mu t}\sum_{i=1}^{3}\bar{\mathcal{N}}(\chi_i)\dot{\chi}_i$. On the time instant $[t_j,t_{j+1})$, it implies from (62) that

$$\Phi\left(t_{j+1}\right)\leq\zeta\left[\Phi\left(t_j\right)+\int_{t_j}^{t_{j+1}}\Lambda e^{\mu t}dt\right], \tag{66}$$

where $\Lambda=\Theta+\sum_{i=1}^{3}\bar{\mathcal{N}}(\chi_i)\dot{\chi}_i$. On the instant $[0,T]$, iterating the inequality (66) from $j=0$ to $j=N_\sigma(T,0)-1$, it induces

$$\begin{aligned}\Phi(T^-)\leq&\,\Phi(t_{N_\sigma(T,0)})+\int_{t_{N_\sigma(T,0)}}^{T}\Lambda e^{\mu t}dt\\\leq&\,\zeta\Bigg[\Phi(t_{N_\sigma(T,0)-1})+\int_{t_{N_\sigma(T,0)-1}}^{t_{N_\sigma(T,0)}}\Lambda e^{\mu t}dt\\&+\zeta^{-1}\int_{t_{N_\sigma(T,0)}}^{T}\Lambda e^{\mu t}dt\Bigg]\leq\cdots\\\leq&\,\zeta^{N_\sigma(T,0)}\Bigg[\Phi(0)+\sum_{j=0}^{N_\sigma(T,0)-1}\zeta^{-j}\int_{t_j}^{t_{j+1}}\Lambda e^{\mu t}dt\\&+\zeta^{-N_\sigma(T,0)}\int_{t_{N_\sigma(T,0)}}^{T}\Lambda e^{\mu t}dt\Bigg].\end{aligned} \tag{67}$$

By utilizing $\tau_a>\frac{\log\zeta}{\mu}$, for $\forall a\in(0,\mu-\frac{\log\zeta}{\mu})$, one gets $\tau_a>\frac{\log\zeta}{\mu-a}$. In addition, based on Definition 1, one has $N_\sigma(T,t)\leq N_0+\frac{(\mu-a)(T-t)}{\log\zeta}$ for $\forall T\geq t\geq 0$. Thus, under the inequality $N_\sigma(T,0)-j\leq 1+N_\sigma(T,t_{j+1})$ with $j=0,1,\ldots,N_\sigma(T,0)$, it yields

$$\zeta^{N_\sigma(T,0)-j}\leq\zeta^{1+N_0}e^{(\mu-a)(T-t_{j+1})}. \tag{68}$$

Furthermore, for $t\in[t_j,t_{j+1})$, since $a<\mu$, it induces

$$\int_{t_j}^{t_{j+1}}\Theta e^{\mu t}dt\leq e^{(\mu-a)t_{j+1}}\int_{t_j}^{t_{j+1}}\Theta e^{at}dt \tag{69}$$

and

$$\begin{aligned}&\int_{t_j}^{t_{j+1}}\bar{\mathcal{N}}(\chi_i)\dot{\chi}_ie^{\mu t}dt\leq\int_{\chi_i(t_j)}^{\chi_i(t_{j+1})}\left|\bar{\mathcal{N}}(\chi_i)\right|e^{\mu t}d\chi_i\\&\leq e^{(\mu-a)t_{j+1}}\int_{\chi_i(t_j)}^{\chi_i(t_{j+1})}\left|\bar{\mathcal{N}}(\chi_i)\right|e^{at}d\chi_i.\end{aligned} \tag{70}$$

Combining (67)-(70) results in

$$\begin{aligned}\Phi\left(T^-\right)\leq&\,\zeta^{N_\sigma(T,0)}\Phi(0)+\zeta^{1+N_0}e^{(\mu-a)T}\Bigg[\int_0^T\Theta e^{at}dt\\&+\sum_{i=1}^{3}\int_{\chi_i(0)}^{\chi_i(T)}\left|\bar{\mathcal{N}}(\chi_i)\right|e^{at}d\chi_i\Bigg].\end{aligned} \tag{71}$$

Under the definition of $\Phi(t)$, one obtains for $\forall T>0$,

$$\begin{aligned}V_{\sigma(T^-)}\left(X\left(T^-\right)\right)\leq&\; e^{N_0\log\zeta}e^{\left(\frac{\log\zeta}{\tau_a}-\mu\right)T}\overline{\alpha}(\|X\|)\\&+\zeta^{1+N_0}\left(\frac{\Theta}{a}+e^{-aT}\sum_{i=1}^{3}\int_{\chi_i(0)}^{\chi_i(T)}\left|\bar{\mathcal{N}}(\chi_i)\right|e^{at}d\chi_i\right).\end{aligned} \tag{72}$$

It can be concluded that if τ_a satisfies $\tau_a>\frac{\log\zeta}{\mu}$, one gets

$$\frac{V_{\sigma(T^-)}(X(T^-))}{\zeta^{1+N_0}}\leq\sum_{i=1}^{3}\int_{\chi(0)}^{\chi(T)}\left|\bar{\mathcal{N}}(\chi_i)\right|d\chi_i+\pi_0 \tag{73}$$

based on $0<e^{-a(T-t)}\leq 1$, where $\pi_0=\frac{1}{\zeta^{1+N_0}}[e^{N_0\log\zeta}\overline{\alpha}(\|X(0)\|)+\zeta^{1+N_0}\frac{\Theta}{a}]$. Here, $\bar{\mathcal{N}}(\chi_i)$ is a Nussbaum gain function. According to Lemma 2, for $\forall T_f>0$, the boundeness of $\chi_i(T)$ for $i=1,2,3$ can be verified on $[0,T_f)$. Furthermore, for $\forall T_f>0$, one has $V_{\sigma(T)}(X(T))$ and $\int_{\chi(0)}^{\chi(T)}\left|\bar{\mathcal{N}}(\chi_i)\right|d\chi_i$ for $i=1,2,3$ are bounded on $[0,T_f)$. Therefore, it can be concluded that if the ADT satisfies $\tau_a>\frac{\ln\zeta}{\mu}$, then ε_2, ε_3, z_1, z_2, z_3, $\tilde{\theta}_1$, $\tilde{\theta}_2$, $\tilde{\theta}_3$, ϖ_1, ϖ_2, and ϖ_3 are bounded for any bounded initial values. Together with (17) and (24), $\tilde{\varepsilon}$ is bounded. To estimate some terms on the right side of (15), the following proposition is provided for the boundedness of all the signals in the closed-loop switched system, whose proof is placed in the Appendix.

Proposition 1: For the dynamic reduced-order switched state observer (13), under the boundedness of y, r, $\dot{r}$ and $\tilde{\varepsilon}$ on $[0,T_f)$, the states ξ, ϕ, φ, γ, $\hat{x}$ and x are bounded on $[0,T_f)$.

According to Proposition 1, all the signals in the closed-loop switched system are bounded on $[0,T_f)$. Based on Lemma 3, the above discussion is true for $T_f=+\infty$. Hence, for the bounded initial conditions, all signals in the closed-loop switched system are bounded under a set of switching signals with ADT satisfying $\tau_a>\frac{\ln\zeta}{\mu}$.

2) Denote $\bar{o}_1=\sup\{\sum_{i=1}^{3}\left|\bar{\mathcal{N}}(\chi_i)\right|\dot{\chi}_i\}$. Then, one gets

$$\begin{aligned}&e^{-aT}\sum_{i=1}^{3}\int_{\chi_i(0)}^{\chi_i(T)}\left|\bar{\mathcal{N}}(\chi_i)\right|e^{at}d\chi_i\\&\leq e^{-aT}\sum_{i=1}^{3}\int_0^T\left|\bar{\mathcal{N}}(\chi_i)\right|e^{at}\dot{\chi}_idt\\&\leq\frac{\bar{o}_1}{a}(1-e^{-aT})\leq\frac{\bar{o}_1}{a}.\end{aligned} \tag{74}$$

According to (72) and (74), one can obtain

$$\frac{1}{2}z_1^2(T)\leq\bar{o}_2, \tag{75}$$

where $\bar{o}_2=e^{N_0\log\zeta}e^{\left(\frac{\log\zeta}{\tau_a}-\mu\right)T}\overline{\alpha}(\|X(0)\|)+\zeta^{1+N_0}\frac{\Theta+\bar{o}_1}{a}$. Together with $\tau_a>\frac{\ln\zeta}{\mu}$ and the definition of z_1 in (28), it yields

$$\lim_{t\to\infty}y^2(t)=\lim_{t\to\infty}z_1(t)^2\leq\bar{o}_3, \tag{76}$$

Authorized licensed use limited to: UNIVERSITY OF VICTORIA. Downloaded on February 27,2024 at 21:29:31 UTC from IEEE Xplore. Restrictions apply.
© 2024 IEEE. Personal use is permitted, but republication/redistribution requires IEEE permission. See https://www.ieee.org/publications/rights/index.html for more information.

This article has been accepted for publication in IEEE Transactions on Vehicular Technology. This is the author's version which has not been fully edited and content may change prior to final publication. Citation information: DOI 10.1109/TVT.2024.3370094

where $\bar{o}_3 = 2(e^{N_0 \log \zeta}\overline{\alpha}(\|X(0)\|) + \zeta^{1+N_0}\frac{\Theta+\bar{o}_1}{a})$. It is clear from (76) that the system output with the unknown measurement sensitivity can stay in a small neighbourhood of zero by choosing appropriately designed parameters. The proof has been completed. ∎

Remark 2: A guideline from Steps I to IV for the proposed output-feedback control scheme is given to clarify the parameter design.

Step I: Select the proper parameters $l_{2,k}$ and $l_{3,k}$, such that the matrix A_k is Hurwitz. Choose the proper parameters ν_k and ϱ_k. Then, a symmetric matrix $P_k > 0$ can be calculated by solving the inequalities (5) and (6).

Step II: Decide the number of neural network nodes and Gaussian functions, then determine the neural network (10).

Step III: Select appropriate controller parameters ω_k, ς, c_i, ℓ_i, a_i, κ_i, and $d_{i,k}$, for $i = 1, 2, 3$ and $k \in \Gamma$, and then determine the controllers (35), (43), and (51) with the adaptive laws (36), (44), and (52).

Step IV: Determine the designed parameters of ADT $\mu > 0$ in (55) and $\zeta \geq 1$ in (56).

IV. Case Studies

This section provides the case studies to show the flexibility and effectiveness of the proposed adaptive output feedback fault-tolerant control scheme on the switched vehicle active suspension delayed system.

Here, the switched vehicle active suspension delayed system consists of two subsystems, where $\sigma(t) : [0, \infty) \to \Gamma = \{1, 2\}$. The parameters of the switched vehicle active suspension delayed system are chosen as $M_v = 350$ kg, $M_u = 40$ kg, $c_s = 1000$ N $\cdot$ s/m, $c_w = 200000$ N/m, $c_r = 100$ N $\cdot$ s/m, $R_1 = 30\ \Omega$, $R_2 = 28\ \Omega$, $L_1 = 40$ H, and $L_2 = 35$ H. In addition, the unknown system parameter is selected as $c_a = 20000$ N/m, $c_e = 20$, $P_e = 2$, $\tau(t) = 0.1(1 + \sin^2(t))$, and $\rho = 0.8$. Then, the parameters of the controller are selected as $l_{2,1} = 20$, $l_{3,1} = 10$, $l_{2,2} = 18$, $l_{3,2} = 15$, $\nu_1 = 2$, $\varrho_1 = 10$, $\nu_2 = 2.2$, $\varrho_2 = 8$, $\omega_1 = 1$, $\omega_2 = 1.2$, $\varsigma = 0.5$, $c_1 = 0.2$, $c_2 = 0.2$, $c_3 = 0.2$, $\ell_1 = 0.1$, $\ell_2 = 0.1$, $\ell_3 = 0.1$, $a_1 = 0.5$, $a_2 = 0.2$, $a_3 = 0.5$, $\kappa_1 = 5$, $\kappa_2 = 5$, $\kappa_3 = 5$, $d_{1,k} = 0.6$, $d_{2,k} = 1.1$, and $d_{3,k} = 1.1$ for $k \in \Gamma$. Meanwhile, based on Lemma 1, the symmetric positive definite matrices can be obtained as follows:

$$P_1 = \begin{bmatrix} 1.152 & -0.265 \\ -0.265 & 0.449 \end{bmatrix}, P_2 = \begin{bmatrix} 1.149 & -0.230 \\ -0.230 & 0.399 \end{bmatrix}.$$

To proceed, the basis function vectors $S_1(X_1)$, $S_2(X_2)$, $S_3(X_3)$ contain 15, 22, and 30 nodes, and their centres ϑ_1, ϑ_2, ϑ_3 evenly spaced in $[-2, 2] \times [-2, 2] \times [-7, 5] \times [-8, 6] \times [-4, 7]$, $[-2, 2] \times [-8, 8] \times [-3, 3] \times [-7, 5] \times [-2, 7] \times [-6, 5]$, $[-11, 5] \times [-2, 2] \times [-7, 5] \times [-8, 6] \times [-4, 7] \times [-5, 7]$ and widths $\iota_1 = 2$, $\iota_2 = 2.5$, $\iota_3 = 4$, respectively. And the faults of the switched delayed electromagnetic actuator are modelled as

$$u_k = \begin{cases} \hbar v_k + b_{1,k}(t), & 1 \leq t \leq 2, \\ \hbar v_k + b_{2,k}(t), & 5 \leq t \leq 8, \\ \hbar v_k + b_{3,k}(t), & 15 \leq t \leq 20, \\ \hbar v_k, & \text{others}, \end{cases} \tag{77}$$

where $\hbar = 0.5$, $b_{1,k}(t) = 0.03\sin(4\pi t)$, $b_{2,k}(t) = 0.2\cos(3\pi t)$, and $b_{3,k}(t) = 0.01\sin(6\pi t)$ for $k \in \Gamma$.

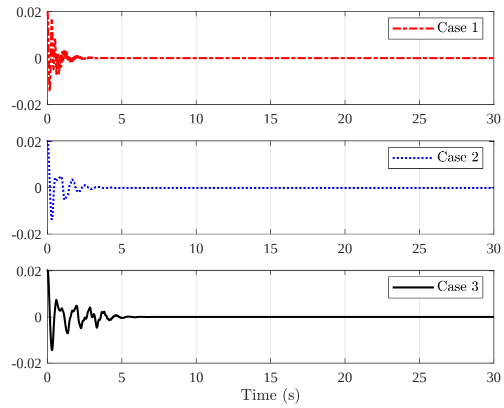

Fig. 4: The suspension space x_1 of Cases 1-3.

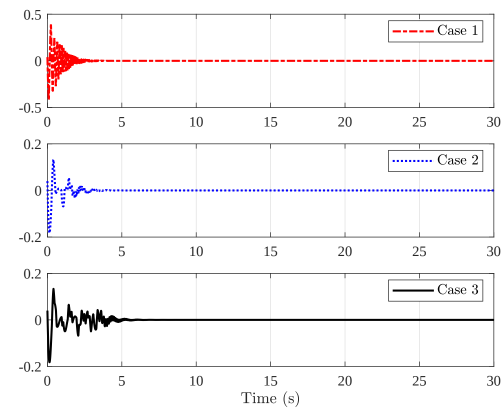

Fig. 5: The relative vertical velocity x_2 of Cases 1-3.

A. Performances of the Proposed Control Strategy

Derived from Theorem 1, all the signals are bounded in the resulting closed-loop system under a set of switching signals with ADT satisfying $\tau_a = 6.31 > \frac{\ln 3.53}{0.20}$. The initial vectors are provided as $x_1(t_0) = 0.02$, $x_2(t_0) = 0.04$, $x_3(t_0) = 0.02$, $\hat{\theta}_1(t_0) = 0.05$, $\hat{\theta}_2(t_0) = 0.1$, $\hat{\theta}_3(t_0) = 0.3$, $r(t_0) = 1$, $\chi_1(t_0) = 0.02$, $\chi_3(t_0) = 0.01$, and others are chosen as zero. In order to test the proposed control strategy, three cases are considered as follows:

Case 1: Consider the vehicle driving on the even ground, i.e., $D_r = 0$ and the boundedness conditions of the uninterrupted contact from wheels to the road surface are selected as $D_1 = 0.001$ and $D_2 = 0.001$;

Authorized licensed use limited to: UNIVERSITY OF VICTORIA. Downloaded on February 27,2024 at 21:29:31 UTC from IEEE Xplore. Restrictions apply.
© 2024 IEEE. Personal use is permitted, but republication/redistribution requires IEEE permission. See https://www.ieee.org/publications/rights/index.html for more information.

This article has been accepted for publication in IEEE Transactions on Vehicular Technology. This is the author's version which has not been fully edited and content may change prior to final publication. Citation information: DOI 10.1109/TVT.2024.3370094

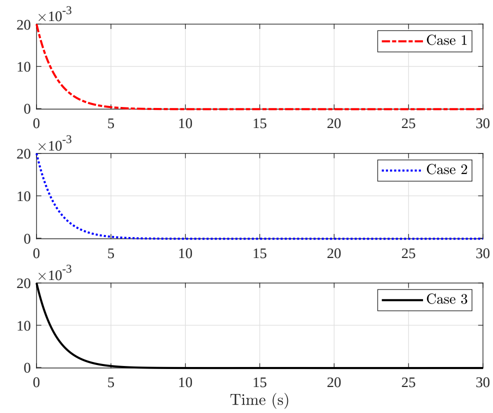

Fig. 6: The electric current intensity x_3 of Cases 1-3.

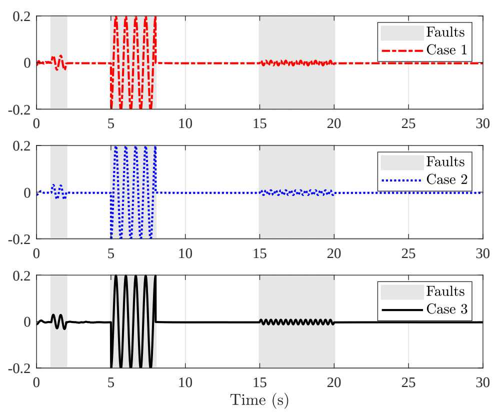

Fig. 7: The designed control input u_k under actuator faults of Cases 1-3.

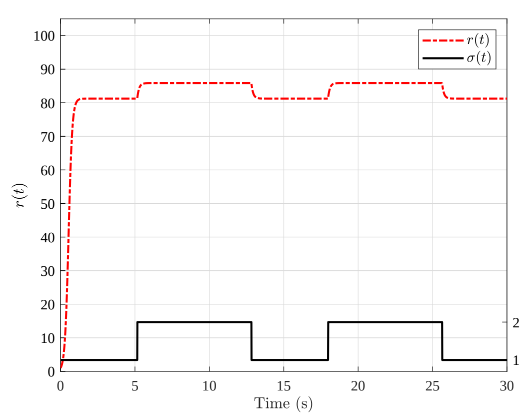

Fig. 8: The dynamic switched gain $r(t)$ and the switching signal $\sigma(t)$.

Case 2: Consider the vehicle driving on the even ground, i.e., $D_r = 0$ and the boundedness conditions of the uninterrupted contact from wheels to the road surface are selected as $D_1 = 0.0001$ and $D_2 = 0.0001$;

Case 3: Consider the vehicle driving on the bumpy ground, i.e.,

$$D_r = \begin{cases} \frac{h_r}{2}\left(1 - \cos\left(\frac{2\pi v_s}{L_b}t\right)\right), & 0 \le t \le 3, \\ 0, & \text{others}, \end{cases} \tag{78}$$

where h_r is the height of the pavement, v_s stands for the velocity of the vehicle, and L_b expresses the length of the pavement. Here, these parameters are selected as $h_r = 0.004$ m, $v_s = 40$ km/h, and $L_b = 7$ m. The boundedness conditions of the uninterrupted contact from wheels to the road surface are selected as $D_1 = 0.0001$ and $D_2 = 0.0001$.

The test results of Cases 1-3 are described in Figs. 4-8. The suspension space of Cases 1-3 can be stabilized in the original region in Fig. 4. The relative vertical velocity response of Cases 1-3 is exhibited in 5. The electric current intensity of Cases 1-3 is shown in Fig. 6. The control input of Cases 1-3 is illustrated in Fig. 7. Furthermore, Fig. 8 displays the dynamic gain of the reduced-order switched state observer under a set of switching signals with ADT. Compared with Cases 1 and 2, the damping element from the active suspension systems can induce some oscillations at the start of the simulation, which are then gradually mitigated by the action of the proposed controller. Compared with Cases 2 and 3, the different road surface conditions may lead to different transient oscillatory behaviors in the system at the beginning. Finally, it is clear that all signals in the closed-loop system are bounded with the random road surface excitation over time with ADT.

B. Comparison with Other Control Strategies

In what follows, we demonstrate the effectiveness of the proposed method compared with the state feedback control scheme in [29] and the full-order observer-based output feedback control scheme in [13]. Additionally, the initial values are the same as the aforementioned ones in Case 3. Also, the road surface excitation is considered as the same situation in Case 3. The compared results of the different strategies are shown in Figs. 9-12.

The suspension space of the different strategies is displayed in Fig. 9. The relative vertical velocity response of the different strategies is shown in 10. The electric current intensity of the different strategies is shown in Fig. 11. The control input of the different strategies is shown in Fig. 12. In Figs. 9 and 12, it can be observed that the convergence rate of the state-feedback control scheme is faster than that of the proposed method; however, this comes at the expense of the state feedback control scheme generating a larger overshoot under a greater control input magnitude compared with the proposed method. In addition, the proposed method exhibits a lower oscillation frequency while concurrently demonstrating a quicker convergence speed. Therefore, compared with the other two control strategies, the proposed reduced-order observer-based output feedback control scheme has a better performance for the vehicle active suspension delayed system.

V. Conclusion

This paper proposes a dynamic output feedback adaptive fault-tolerant control strategy for the switched vehicle active

Authorized licensed use limited to: UNIVERSITY OF VICTORIA. Downloaded on February 27,2024 at 21:29:31 UTC from IEEE Xplore. Restrictions apply.
© 2024 IEEE. Personal use is permitted, but republication/redistribution requires IEEE permission. See https://www.ieee.org/publications/rights/index.html for more information.

This article has been accepted for publication in IEEE Transactions on Vehicular Technology. This is the author's version which has not been fully edited and content may change prior to final publication. Citation information: DOI 10.1109/TVT.2024.3370094

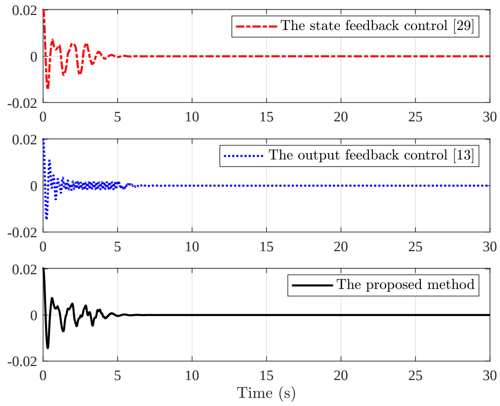

Fig. 9: The suspension space x_1 of the different strategies.

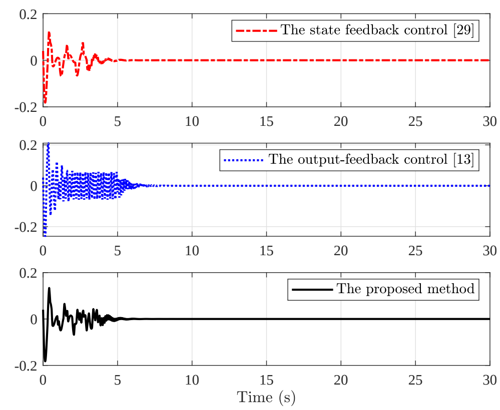

Fig. 10: The relative vertical velocity x_2 of the different strategies.

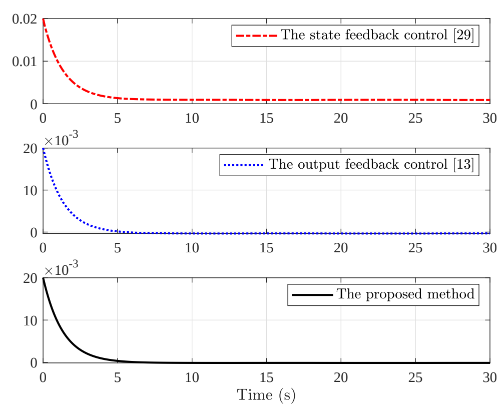

Fig. 11: The electric current intensity x_3 of the different strategies.

suspension delayed system in the presence of the unknown measurement sensitivity from the system output. By utilizing the information from the systems output and the actuator's delayed input, the switched reduced-order state observer is constructed to compensate for the unavailable states with a dynamic switched gain. It is demonstrated that the effect of the actuator input delay and fault can be compensated by the

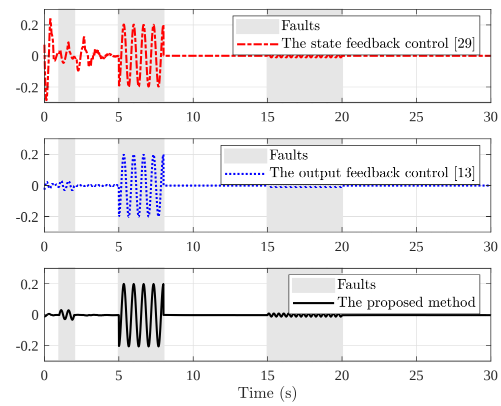

Fig. 12: The designed control input u_k under actuator faults of the different strategies.

switched auxiliary systems via the backstepping technique. Based on the Nussbaum gain technique and the multiple Lyapunov functions, the proposed dynamic output feedback fault-tolerant control scheme can ensure that all the signals in the closed-loop system are semi-globally uniformly ultimate bounded, and its relative vertical displacement stays in the small zero neighbourhood under a set of switching signals with ADT. Finally, the flexibility and effectiveness of the proposed control approach have been illustrated by the case studies. In the next work, the output-feedback control problem of global stabilization will be investigated for switched semi-vehicle or full-vehicle active suspension systems under asynchronous switching with mode-dependent or edge-dependent ADT.

APPENDIX

Proof of Proposition 1: Under a transformation $\tilde{\phi}_i = r^{2-i-\varrho_k}\phi_i$ with $\tilde{\phi} = [\tilde{\phi}_2, \tilde{\phi}_3]^\top$, the boundedness of ϕ will be verified as follows. Consider the Lyapunov function as $V_{\tilde{\phi}} = \tilde{\phi}^\top P_k \tilde{\phi}$. Then, it induces a similar result from (26) that

$$\begin{aligned}\dot{V}_{\tilde{\phi}} \leq\ & 2\tilde{\phi}^\top P_k K_{1,k} r^{2-\varrho_k} y - 2\tilde{\phi}^\top P_k K_2 r^{-\varrho_k}\dot{r}y \\ & - \underline{\omega}_k \tilde{\phi}^\top P_k \tilde{\phi} - \varsigma\|\tilde{\phi}\|^2 \\ \leq & \frac{1}{\varsigma_1}\|P_k K_{1,k}\|^2 r^{4-2\varrho_k} y^2 + \frac{1}{\varsigma_2}\|P_k K_2\| r^{-2\varrho_k}\dot{r}^2 y^2 \\ & - \underline{\omega}_k \tilde{\phi}^\top P_k \tilde{\phi} - (\varsigma - \varsigma_1 - \varsigma_2)\|\tilde{\phi}\|^2, \end{aligned} \tag{79}$$

where $K_{1,k} = [l_{3,k}, 0]^\top$ and $K_2 = [1, 2]^\top$ are parameter vectors. According to the definition of $\tilde{\theta}_i$ for $i = 1, 2, 3$, one can know that $\hat{\theta}_i$ is bounded. Then, by (35), (43), and (51), one gets α_i for $i = 1, 2, 3$ is bounded on $[0, T_f)$. Then, from (51), the actual control input υ_k is bounded on $[0, T_f)$. Based on (28), y, γ_2 and γ_3 are bounded on $[0, T_f)$. Meanwhile, x_1 is bounded based on (2). Combined with the boundedness of y, r, and $\dot{r}$, it can be verified from (13) and (79) that ϕ and ξ are bounded on $[0, T_f)$. Similar to (79), the boundedness of φ can be obtained on $[0, T_f)$. To proceed, based on the (14), $\hat{x}$ is bounded on $[0, T_f)$. Thus, according to (15) and the boundedness of $\tilde{\varepsilon}$, one gets x_2 and x_3 are bounded on $[0, T_f)$. The proof has been completed.

Authorized licensed use limited to: UNIVERSITY OF VICTORIA. Downloaded on February 27,2024 at 21:29:31 UTC from IEEE Xplore. Restrictions apply.
© 2024 IEEE. Personal use is permitted, but republication/redistribution requires IEEE permission. See https://www.ieee.org/publications/rights/index.html for more information.

This article has been accepted for publication in IEEE Transactions on Vehicular Technology. This is the author's version which has not been fully edited and content may change prior to final publication. Citation information: DOI 10.1109/TVT.2024.3370094

REFERENCES

[1] H. Kim, W. Yoo, S. Ha, and J. M. Chung, "In-vehicle network average response time analysis for CAN-FD and automotive ethernet," *IEEE Transactions on Vehicular Technology*, vol. 72, no. 6, pp. 6916–6932, 2023.

[2] Q. Zeng and J. Zhao, "Dynamic event-triggered-based adaptive finite-time neural control for active suspension systems with displacement constraint," *IEEE Transactions on Neural Networks and Learning Systems*, 2022, doi: 10.1109/TNNLS.2022.3201695.

[3] C. M. Ho and K. K. Ahn, "Observer based adaptive neural networks fault-tolerant control for pneumatic active suspension with vertical constraint and sensor fault," *IEEE Transactions on Vehicular Technology*, vol. 72, no. 5, pp. 5862–5876, 2023.

[4] M. Zhang, X. Jing, L. Zhang, W. Huang, and S. Li, "Toward a finite-time energy-saving robust control method for active suspension systems: Exploiting beneficial state-coupling, disturbance, and nonlinearities," *IEEE Transactions on Systems, Man, and Cybernetics: Systems*, vol. 53, no. 9, pp. 5885–5896, 2023.

[5] F. Viadero-Monasterio, B. L. Boada, H. Zhang, and M. J. L. Boada, "Integral-based event triggering actuator fault-tolerant control for an active suspension system under a networked communication scheme," *IEEE Transactions on Vehicular Technology*, vol. 72, no. 11, pp. 13 848–13 860, 2023.

[6] H. Chen, Y. J. Liu, L. Liu, S. Tong, and Z. Gao, "Anti-saturation-based adaptive sliding-mode control for active suspension systems with time-varying vertical displacement and speed constraints," *IEEE Transactions on Cybernetics*, vol. 52, no. 7, pp. 6244–6254, 2022.

[7] J. Na, Y. Huang, X. Wu, S. F. Su, and G. Li, "Adaptive finite-time fuzzy control of nonlinear active suspension systems with input delay," *IEEE Transactions on Cybernetics*, vol. 50, no. 6, pp. 2639–2650, 2020.

[8] W. Wu, Z. Peng, D. Wang, L. Liu, and Q. L. Han, "Network-based line-of-sight path tracking of underactuated unmanned surface vehicles with experiment results," *IEEE Transactions on Cybernetics*, vol. 52, no. 10, pp. 10 937–10 947, 2022.

[9] T. Wang and Y. Li, "Neural-network adaptive output-feedback saturation control for uncertain active suspension systems," *IEEE Transactions on Cybernetics*, vol. 52, no. 3, pp. 1881–1890, 2022.

[10] Y. Li, T. Wang, W. Liu, and S. Tong, "Neural network adaptive output-feedback optimal control for active suspension systems," *IEEE Transactions on Systems, Man, and Cybernetics: Systems*, vol. 52, no. 6, pp. 4021–4032, 2022.

[11] S. Yan, W. Sun, X. Yu, and H. Gao, "Adaptive sensor fault accommodation for vehicle active suspensions via partial measurement information," *IEEE Transactions on Cybernetics*, vol. 52, no. 11, pp. 12 290–12 301, 2022.

[12] H. Pan and W. Sun, "Nonlinear output feedback finite-time control for vehicle active suspension systems," *IEEE Transactions on Industrial Informatics*, vol. 15, no. 4, pp. 2073–2082, 2019.

[13] Y. Li, T. Wang, W. Liu, and S. Tong, "Neural network adaptive output-feedback optimal control for active suspension systems," *IEEE Transactions on Systems, Man, and Cybernetics: Systems*, vol. 52, no. 6, pp. 4021–4032, 2022.

[14] J. Lin, K. W. E. Cheng, Z. Zhang, N. C. Cheung, X. Xue, and T. W. Ng, "Active suspension system based on linear switched reluctance actuator and control schemes," *IEEE Transactions on Vehicular Technology*, vol. 62, no. 2, pp. 562–572, 2013.

[15] Z. Li, G. Cao, W. Xie, R. Gao, and W. Zhang, "Switched-observer-based adaptive neural networks tracking control for switched nonlinear time-delay systems with actuator saturation," *Information Sciences*, vol. 621, pp. 36–57, 2023.

[16] Z. Li, D. Yue, Y. Ma, and J. Zhao, "Neural-networks-based prescribed tracking for nonaffine switched nonlinear time-delay systems," *IEEE Transactions on Cybernetics*, vol. 52, no. 7, pp. 6579–6590, 2022.

[17] J. Zhao and D. J. Hill, "On stability, L_2-gain and H_∞ control for switched systems," *Automatica*, vol. 44, pp. 1220–1232, 2008.

[18] Z. Li, L. Long, and J. Zhao, "Linear output-feedback-based semi-global stabilization for switched nonlinear time-delay systems," *Journal of the Franklin Institute*, vol. 356, no. 13, pp. 7224–7245, 2019.

[19] D. Cui, C. K. Ahn, and Z. Xiang, "Fault-tolerant fuzzy observer-based fixed-time tracking control for nonlinear switched systems," *IEEE Transactions on Fuzzy Systems*, vol. 31, no. 12, pp. 4410–4420, 2023.

[20] D. Liberzon, *Switching in Systems and Control*, Boston, MA, USA: Birkhäuser, 2003.

[21] J. Zhang, S. Li, C. K. Ahn, and Z. Xiang, "Adaptive fuzzy decentralized dynamic surface control for switched large-scale nonlinear systems with full-state constraints," *IEEE Transactions on Cybernetics*, vol. 52, no. 10, pp. 10 761–10 772, 2022.

[22] Z. Li and L. Long, "Global stabilization of switched feedforward nonlinear time-delay systems under asynchronous switching," *IEEE Transactions on Circuits and Systems I: Regular Papers*, vol. 67, no. 2, pp. 711–724, 2020.

[23] H. Chen, Z. Liu, C. Alippi, B. Huang, and D. Liu, "Explainable intelligent fault diagnosis for nonlinear dynamic systems: From unsupervised to supervised learning," *IEEE Transactions on Neural Networks and Learning Systems*, 2022, doi: 10.1109/TNNLS.2022.3201511.

[24] J. Xiong, X. H. Chang, J. H. Park, and Z. M. Li, "Nonfragile fault-tolerant control of suspension systems subject to input quantization and actuator fault," *International Journal of Robust and Nonlinear Control*, vol. 30, no. 16, pp. 6720–6743, 2020.

[25] S. Y. Han, J. Zhou, Y. H. Chen, Y. F. Zhang, G. Y. Tang, and L. Wang, "Active fault-tolerant control for discrete vehicle active suspension via reduced-order observer," *IEEE Transactions on Systems, Man, and Cybernetics: Systems*, vol. 51, no. 11, pp. 6701–6711, 2021.

[26] H. Chen and B. Huang, "Fault-tolerant soft sensors for dynamic systems," *IEEE Transactions on Control Systems Technology*, vol. 31, no. 6, pp. 2805–2818, 2023.

[27] Y. Xun, Z. Deng, J. Liu, and Y. Zhao, "Side channel analysis: A novel intrusion detection system based on vehicle voltage signals," *IEEE Transactions on Vehicular Technology*, vol. 72, no. 6, pp. 7240–7250, 2023.

[28] Z. Qi, Q. Shi, and H. Zhang, "Tuning of digital PID controllers using particle swarm optimization algorithm for a CAN-based DC motor subject to stochastic delays," *IEEE Transactions on Industrial Electronics*, vol. 67, no. 7, pp. 5637–5646, 2020.

[29] Y. J. Liu, Q. Zeng, S. Tong, C. L. P. Chen, and L. Liu, "Actuator failure compensation-based adaptive control of active suspension systems with prescribed performance," *IEEE Transactions on Industrial Electronics*, vol. 67, no. 8, pp. 7044–7053, 2020.

[30] L. Liu, Y. J. Liu, D. Li, S. Tong, and Z. Wang, "Barrier lyapunov function-based adaptive fuzzy FTC for switched systems and its applications to resistance-inductance-capacitance circuit system," *IEEE Trans Cybernetics*, vol. 50, no. 8, pp. 3491–3502, 2020.

[31] L. Tang and J. Zhao, "Switched threshold-based fault detection for switched nonlinear systems with its application to Chua's circuit system," *IEEE Transactions on Circuits and Systems I: Regular Papers*, vol. 66, no. 2, pp. 733–741, 2019.

[32] L. Praly and Z. P. Jiang, "Linear output feedback with dynamic high gain for nonlinear systems," *Systems & Control Letters*, vol. 53, no. 2, pp. 107–116, 2004.

[33] S. S. Ge, H. Fan, and L. Tong Heng, "Adaptive neural control of nonlinear time-delay systems with unknown virtual control coefficients," *IEEE Transactions on Systems, Man, and Cybernetics, Part B (Cybernetics)*, vol. 34, no. 1, pp. 499–516, 2004.

[34] B. Jiang, Q. Shen, and P. Shi, "Neural-networked adaptive tracking control for switched nonlinear pure-feedback systems under arbitrary switching," *Automatica*, vol. 61, pp. 119–125, 2015.

[35] L. J. Long and J. Zhao, "Switched-observer-based adaptive neural control of MIMO switched nonlinear systems with unknown control gains," *IEEE Transactions on Neural Networks and Learning Systems*, vol. 28, no. 7, pp. 1696–1709, 2017.

[36] P. Ning, C. Hua, K. Li, and R. Meng, "A blow-up function approach to global event-triggered prescribed tracking output feedback control of nonlinear systems," *IEEE Transactions on Circuits and Systems I: Regular Papers*, vol. 69, no. 10, pp. 4225–4236, 2022.

[37] J. Ma, S. Xu, G. Zhuang, Y. Wei, and Z. Zhang, "Adaptive neural network tracking control for uncertain nonlinear systems with input delay and saturation," *International Journal of Robust and Nonlinear Control*, vol. 30, no. 7, pp. 2593–2610, 2020.

Authorized licensed use limited to: UNIVERSITY OF VICTORIA. Downloaded on February 27,2024 at 21:29:31 UTC from IEEE Xplore. Restrictions apply.
© 2024 IEEE. Personal use is permitted, but republication/redistribution requires IEEE permission. See https://www.ieee.org/publications/rights/index.html for more information.

This article has been accepted for publication in IEEE Transactions on Vehicular Technology. This is the author's version which has not been fully edited and content may change prior to final publication. Citation information: DOI 10.1109/TVT.2024.3370094

Zhenhua Li received the B.S. degree in automation from Harbin University of Science and Technology, Harbin, China, in 2017, and the M.S. degree in control theory and control engineering from Northeastern University, Shenyang, China, in 2020. He is currently pursuing the Eng.D. degree in electronic information at the Department of Automation, Shanghai Jiao Tong University, Shanghai, China.

His research interests include adaptive control, nonlinear systems, observer theory, switched systems, and time-delay systems.

Dr. Li was a recipient of the Best Theory Paper Award at the China Automation Congress from Chinese Association of Automation (CAA) in 2022. He serves as a reviewer of some international journals such as IEEE TRANSACTIONS ON INDUSTRIAL INFORMATICS, INTERNATIONAL JOURNAL OF SYSTEMS SCIENCE, etc.

Hongtian Chen (Member, IEEE) received his Ph.D. degree in College of Automation Engineering from Nanjing University of Aeronautics and Astronautics, China, in 2019. He was a Post-Doctoral Fellow at the University of Alberta, Canada, from 2019 to 2023.

Dr. Chen joined Shanghai Jiao Tong University, China in 2023 as an Associate Professor in the Department of Automation. His research interests include fault diagnosis and fault-tolerant control, data mining and analytics, machine learning, and cooperative control; and their applications in high-speed trains, new energy systems, industrial processes, and autonomous systems.

Dr. Chen was a recipient of the Grand Prize of Innovation Award of Ministry of Industry and Information Technology of the People's Republic of China in 2019, the Excellent Ph.D. Thesis Award of Jiangsu Province in 2020, the Excellent Doctoral Dissertation Award from Chinese Association of Automation (CAA) in 2020, Marie Skłodowska-Curie Actions in 2023, and Pujiang Scholar in 2023. He is an Associate Editor and Guest Editor of several international journals such as IEEE TRANSACTIONS ON INSTRUMENTATION AND MEASUREMENT, IEEE TRANSACTIONS ON ARTIFICIAL INTELLIGENCE, IEEE TRANSACTIONS ON NEURAL NETWORKS AND LEARNING SYSTEMS, INTERNATIONAL JOURNAL OF ROBOTICS AND AUTOMATION, etc. He was also a co-chair and program chair for international conferences such as the 6th International Conference on Robotics, Control and Automation Engineering.

Wentao Wu (Graduated Student Member, IEEE) received the B.E. degree in electrical engineering and automation from the Harbin University of Science and Technology, Harbin, China, in 2018, and the M.E. degree in electrical engineering from Dalian Maritime University, Dalian, China, in 2021. He is currently pursuing the Ph.D. degree in electronic information engineering from Shanghai Jiao Tong University, Shanghai, China.

From 2023 to 2024, he is a Visiting Research Scholar with the Department of Mechanical Engineering, University of Victoria, Victoria, BC, Canada. His current research interests include cooperative control, safety-critical control, and constrained control of multiple marine vehicles.

Weidong Zhang (Senior Member, IEEE) received his B.S., M.S., and Ph.D. degrees from Zhejiang University, Hangzhou, China, in 1990, 1993, and 1996, respectively, and then worked as a Postdoctoral Fellow at Shanghai Jiao Tong University.

He joined Shanghai Jiao Tong University, Shanghai, China, in 1998 as an Associate Professor and has been a Full Professor since 1999. He worked with the University of Stuttgart, Stuttgart, Germany, as an Alexander von Humboldt Fellow from 2003 to 2004. He is a recipient of National Science Fund for Distinguished Young Scholars, China and Cheung Kong Scholar, Ministry of Education, China. He is currently Director of the Engineering Research Center of Marine Automation, Shanghai Municipal Education Commission, and Director of Marine Intelligent System Engineering Research Center, Ministry of Education, China. His research interests include control theory, machine learning theory, and their applications in industry and autonomous systems. He is the author of 265 SCI papers and 1 book, and holds 72 patents.

Authorized licensed use limited to: UNIVERSITY OF VICTORIA. Downloaded on February 27,2024 at 21:29:31 UTC from IEEE Xplore. Restrictions apply.
© 2024 IEEE. Personal use is permitted, but republication/redistribution requires IEEE permission. See https://www.ieee.org/publications/rights/index.html for more information.